ChemComm

Accepted Manuscript

ROYAL SOCIETY OF CHEMISTRY

rsc.li/chemcomm

View Article Online
DOI: 10.1039/C6CC08748E

Journal Name

COMMUNICATION

Elucidating the light-induced charge accumulation in an artificial analogue of methane monooxygenase enzymes using time-resolved x-ray absorption spectroscopy

Received 00th January 20xx,
Accepted 00th January 20xx

DOI: 10.1039/x0xx00000x

www.rsc.org/

Dooshaye Moonshiram,[a*] Antonio Picón,[a] Alvaro Vazquez-Mayagoitia,[b] Xiaoyi Zhang,[c] Ming-Feng Tu,[a] Pablo Garrido-Barros[d],Jean-Pierre Mahy,[e] Frédéric Avenier,[e] and Ally Aukauloo [e,f]

We report the use of time-resolved X-ray absorption spectroscopy in the ns-µs time scale to track the light induced two electron transfer processes in a multi-component photocatalytic system, consisting of $[Ru(bpy)_3]^{2+}$/ a diiron(III,III) model/triethylamine. EXAFS analysis with DFT calculations confirm the structural configurations of the diiron(III,III) and reduced diiron(II,II) states.

Soluble methane monooxygenase (MMOs) enzymes from methanotrophic bacteria found in various anaerobic surroundings such as oceans, lakes and wetlands, can catalyze the oxidation of methane to methanol under ambient conditions.[1-4] Considering the high stability of the C-H bond, the efficient controlled conversion of methane to methanol, a liquid fuel, is a remarkable process that is currently a subject of great industrial importance. Electronic and structural insights obtained from enzymological studies of MMOs could open new avenues for generating renewable energy in an economical and sustainable manner.[5] The general functional scheme of a large variety of non-heme metalloenzymes including MMOs implies the initial activation of a diiron(III,III) core through a two-electron reduction process, by NADH to form a reduced diiron(II,II) state. The reduced diiron(II,II) state can subsequently react with oxygen to form an diiron(III) peroxo species[6] that eventually leads to O-O bond cleavage forming bis(µ-oxo)diiron(IV) species responsible for organic substrate oxidations.[7] Although tremendous efforts have been invested through multiple spectroscopic techniques such as Raman[1], Mossbauer[8], Electron Paramagnetic Resonance[8-10], ENDOR/ESSEM[8, 11] , Magnetic circular dichroism[12, 13], and X-ray absorption spectroscopy[8, 14, 15] to characterize the diiron stable sites and their transient intermediates, the mechanism of dioxygen activation and underlying subsequent oxidation reactions are not fully understood. The intricacies of the protein environment in biological enzymes and identification of key functional iron(III) peroxo, iron(III) hydroxo and iron(IV) oxo species in the catalytic activation of oxygen is a complex undertaking.

During the last decade, systems that combine both a photoactive unit and a molecular catalyst with the target of using light energy for bond breaking and making catalysis at the metal centre, have received much attention.[16-18]

Scheme 1 A. Photocatalytic system consisting of the diiron(III,III) complex described previously[16], $[Ru(bpy)_3]^{2+}$ photosensitizer and the triethylamine electron donor in acetonitrile B. Photo-induced dioxygen activation at diiron(III,III) and subsequent atom transfer adapted from [16]. Red brackets indicate the processes investigated in this study.

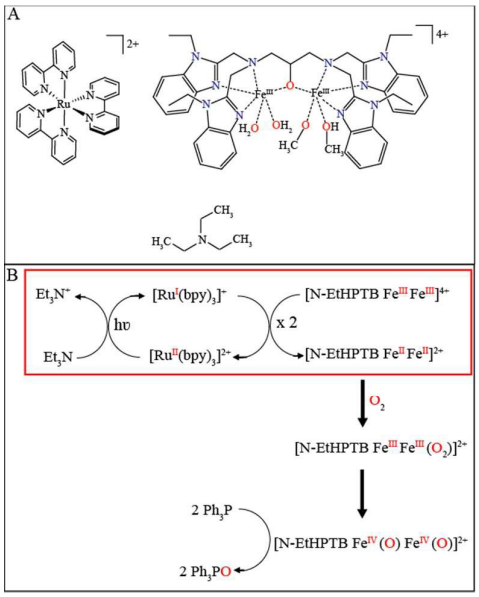

Among those systems, synthetic assemblies consisting of a photosensitizer linked to a catalytic module for dioxygen activation

[a] Chemical Sciences and Engineering Division, [c] X-ray Science Division, Argonne National Laboratory, [b] Argonne Leadership Computing Facility, 9700 S. Cass Avenue, Lemont IL 60439, U.S.A. Email: dmoonshi@gmail.com
[d] Institute of Chemical Research of Catalonia (ICIQ), Avgda. Països Catalans, 16, 43007 Tarragona, Spain
[e] Institut de Chimie Moléculaire et des Matériaux d'Orsay(UMR CNRS 8182), Bat 420, Rue Doyen G. Poitou, Université Paris-Sud, Orsay 91405, France
[f] Service de Bioénergétique, Biologie Structurale et Mécanismes (SB_2SM), CEA, iBiTec-S Biochimie Biophysique et Biologie Structurale (B_3S), I_2BC, UMR 9198, F-91191 Gif-sur-Yvette, France
† Electronic Supplementary Information (ESI) available: Details of Materials and methods, EXAFS fits and DFT calculated parameters are available. See DOI: 10.1039/x0xx00000x

View Article Online
DOI: 10.1039/C6CC08748E

such as diiiron or mononuclear copper centers have also emerged.[16, 19] A well-characterized diiron(III,III) complex based on the biscompartmental ligand abbreviated as N-EtHPTB for the N,N,N',N'-tetrakis(N-ethyl-2-benzimidazolylmethyl)-2hydroxy-1,2-diaminopropane)[16] was associated in acetonitrile solution with the commonly known $[Ru(bpy)_3]^{2+}$ photosensitizer and triethylamine as electron donor (Scheme 1). Interestingly, under sequential light illumination and exposition to dioxygen, the triptych mixture was found to perform a catalytic oxygen atom transfer reaction. A mechanistic proposal was put forward based on the light-activated formation of the diiron(II,II) species capable of contributing toward oxygen activation to generate a diiron(III)-μ-1,2-peroxo intermediate that could in turn transfer an oxygen atom to a substrate (Scheme 1B).

However, previous optical studies[16] conducted with the $[Ru(bpy)_3]^{2+}$ chromophore could not distinguish the reduced diiron(II,II) from the diiron(III,III) state as their electronic signatures were masked by the high extinction coefficients and spectral absorption window of the photoactive counterpart. Also, as previously shown[20], non-heme iron sites with even electron integer spin (high spin S= 2) and non-Kramer ions cannot be easily detected by traditional EPR techniques. Strong ligand to Fe^{II} charge transfer transitions are additionally located at higher photon energies (< 30 000 cm^{-1}) thus precluding its observation in the accessible region of the optical absorption spectrum. In this work, we ascertain the formation of the diiron(II,II) species capable of forming a peroxo species through the powerful time-resolved pump (laser), probe (X-ray) absorption spectroscopy technique (tr-XAS).

The necessity to observe the dynamics of electron transfer processes in real time and retrieve the electronic and structural information of the involved transient states is critical for advancing our knowledge of the underlying mechanism. Tr-XAS with picosecond-microsecond time resolution has been used to capture snapshots of those transient states in many photocatalytically relevant complexes.[21, 22] In this scenario, a laser pulse (pump) initiates a photochemical reaction within the system under study and an x-ray pulse (probe) at varying delays is used to interrogate the local electronic and structural change. Therefore using tr-XAS technique to track such subtle changes in molecular systems in solution phase has considerably enhanced our fundamental understanding of photochemical events, solar energy conversion interfacial electron transfer and biological enzymatic systems.[21-24]

With this mind set, we demonstrate herein the light induced electron transfer dynamics leading to the reduction of the diiron(III,III) ground state. Extended X-ray absorption fine structure (EXAFS) analyses in combination with Density Functional Theory (DFT) calculations are used to reveal important structural information about the diiron(III,III) and diiron(II,II) states.

We studied the formation and decay of the diiron(II) containing complex mixture in two different scenarios: a multimolecular system consisting (i) a binary mixture of the photosensitizer $[Ru(bpy)_3]^{2+}$ (10 mM) and diiron(III,III) complex (1 mM)(Figure 1 A) in acetonitrile (ii) a ternary mixture of $[Ru(bpy)_3]^{2+}$ (10 mM), diiron(III,III) complex) (1 mM) with triethylamine as the sacrificial electron donor (660 mM) (Figure 2 A) in acetonitrile.

The solution mixtures were pumped at 527 nm wavelength using a regenerative amplified laser with 1.6 kHz repetition rate. The sample was circulated through a stainless steel nozzle into a free-flowing 550 μm cylindrical jet inside an airtight aluminium chamber and continuously degassed with nitrogen. (See SI for more details). Care was also taken to vigorously degas the solution mixtures prior to laser excitation due to the air sensitivity of the diiron(II,II) state. As a control measurement, the XANES spectra of the diiron(III,III) complex in the absence of both the photosensitizer and triethylamine electron donor was carried out in the presence of both the laser and X-ray beams . No change was observed in the X-ray absorption near edge (XANES) spectra of diiron(III,III) over the course of around 4 hrs (Figure S1). This result thus clearly rules out the direct photoreduction of diiron(III,III) that could occur due to side reactions following radiolysis of the solvent. Upon light excitation of the $[Ru(bpy)_3]^{2+}$, metal-to-ligand charge transfer triggers electron transfer to form a reduced diiron(II,II) species (Figure 1 B, C). This is characterized by a shift of the XANES edge energy toward lower energies. The features in the tr-XAS spectrum obtained by subtracting the laser-on and laser-off spectrum provide information about the evolving transient states involved in the binary mixture. A prominent rising peak at 7124 eV together with a broad dip at 7141 eV corresponds to the partial formation of the reduced diiron(II,III) species and the ground state bleaching of diiron(III,III) respectively (Figure,1 C). The blue spectrum shown in Figure 1 B corresponds to the formation of pure diiron(II,II) obtained in a ternary mixture as will be discussed below. This is further used as a reference for EXAFS analysis.

The tr-XAS spectra at averaged delays ranging between 230 ns-30 μs for the binary mixture are shown in Figure 1 C. The kinetics for the formation of diiron(II,III) is monitored at the peak energy, 7124 eV, of the transient signal (Figure 1 C). A quick rise in the order of 286±8 ns indicates the fast charge transfer from the excited photosensitizer to form the reduced diiron(II,III) species whereas the slow decay of 13.0 ± 0.3 μs indicates a slower recombination with the oxidized form of the photosensitizer (Figure 1 D).

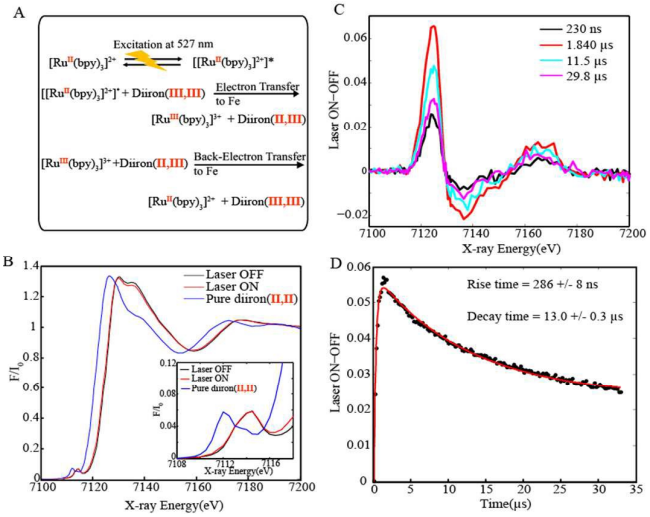

Figure 1 A. Scheme of processes taking place in the tr-XAS experiment **B.** Experimental transient X-ray absorption spectrum for $[Ru(bpy)_3]^{2+}$ (10mM)/diiron(III,III) (1 mM) binary mixture in acetonitrile measured before (black) and an averaged time delay of 1.8 μs after laser excitation(red). Pure diiron(II,II) obtained through

View Article Online
DOI: 10.1039/C6CC08748E

a ternary mixture with excess electron donor in acetonitrile is also shown (blue). **C**) Pump-probe time delay scans recorded at 7124 eV of a binary mixture, corresponding to the formation and decay of the diiron(II,III) photo-induced species. **D**) Experimental (laser on-laser off) spectrum corresponding to diiron(II,III) transient signal at varying time delays.

Interestingly, as previously mentioned, the decay kinetics of the diiron(II,III) species was significantly slowed down in the presence of triethylamine as the sacrificial electron donor (Figure 2 B). The lifetime of the mixed diiron(II,III) species being formed in the ternary mixture is longer than the pulse period of the ultrafast laser being used (Please see SI) such that each successive laser pulse is able to further reduce the recirculating mixed diiron(II) containing complex mixture. Therefore, more of the diiron(III,III) mixture being formed is reduced, until eventually nearly all of the complex is in the diiron(II,II) state, thus enabling its structural determination (Figure 2B, C). The full conversion of the diiron(II,II) state was achieved within *ca.* 20 min followed by its much longer decay time in the order of 20.0 ± 3.4 hours (Figure 2C). The Fe K-edge energy at normalized fluorescence 0.5, of the diiron(II,II) state is around 7120 eV consistent with the presence of pure Fe^{II} as previously observed in XANES measurements of non-heme iron(II) complexes with similar energy calibration.[25, 26] Moreover, the purity of the diiron(II,II) state was determined by comparing its XANES spectrum to diiron(III,III). A relative shift in energy of 3.5 eV is obtained which based on the comparison of non-heme iron complexes[25, 26] with similar structural environments, confirms the presence of nearly pure diiron(II,II)in the ternary mixture with excess of the electron donor.

Comparison of the diiron(II,III) reduced complex mixture in a binary mixture with that obtained in the ternary mixture showed the presence of 9 % pure diiron(II,II) or 18 % diiron(II,III) (Figure S2). Since only a maximum relative shift in energy of ~0.32 eV for the reduced iron(II) species was observed in the binary mixture, the presence of the diiron(II,III) dimer is naturally dominated in the latter case. This confirms the favored back electron transfer between the reduced diiron(II,III) state and the oxidized form of the photosensitizer, $[Ru(bpy)_3]^{3+}$ in the binary mixture as shown in Figure 1A.

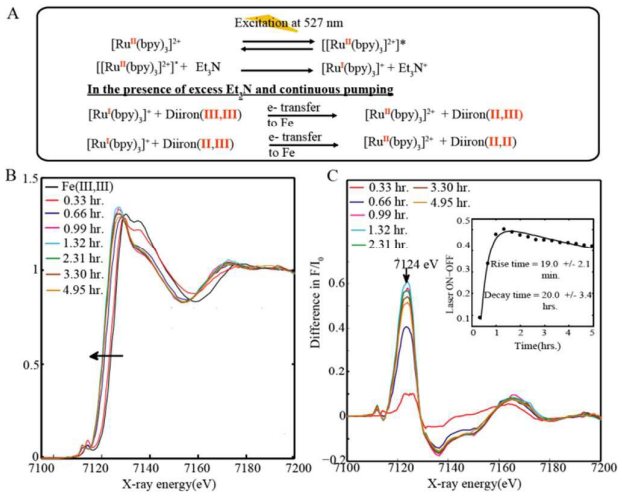

Figure 2 A. Scheme of processes taking place in the tr-XAS experiment **B.** Experimental transient X-ray absorption spectrum for $[Ru(bpy)_3]^{2+}$ (10mM)/diiron(III,III)complex (1 mM) and triethylamine (660mM) ternary mixture measured under continuous light excitation in acetonitrile. **C)** Experimental (laser on-laser off) corresponding to the diiron(II) complex mixture's transient signal at varying delays for a complete photocatalytic system.

Figure 1 B shows the pre-edge features of diiron(III,III) and diiron(II,II) corresponding to the 1s to 3d quadrupole transitions and dipole excitations of the core electrons into the valence 3d states hybridized with ligand p orbitals.[27, 28] The pre-edge intensity due to metal 4 p mixing into 3 d orbitals has been shown to increase with decrease in the coordination number due to an increase in the dipole allowed 1s→ 4 p character contributing to this transition.[27] In this case, minor differences are observed in the pre-edge intensity of diiron(III,II) and pure diiron(II,II) (Figure 1 B) pointing towards the lack of ligand loss or coordination number change as further confirmed through geometry optimization calculations (Table S2, SI).

Moreover, the large difference in the kinetics for the decay of the diiron(II,III) state in a ternary mixture shows that the reductive quenching of the excited photosensitizer is the predominant photocatalytic pathway followed by electron transfer to the diiron(III,III) state. These results are consistent with the typical pathway observed in the presence of high amounts of the electron donor, and confirm previous optical transient absorption measurements carried out on the multimolecular ternary mixture whereby the reduced form of the photosensitizer, the formal $[Ru^{I}(bpy)_3]^{+}$ species was observed .[16] In the presence of an excess of triethylamine; the excited Ru* first reacts with the electron donor to form the reduced state of Ru*. The presence of the long lived highly reducing form of the chromophore enhances the electron transfer process to the diiron(III,III) catalytic module enabling the formation of the nearly pure diiron(II,II) state. As such, this study clearly demonstrates the two electron transfer activation of the diiron(III,III) and stands as a rare example of the characterization of multiple electron transfer process using tr-XAS.

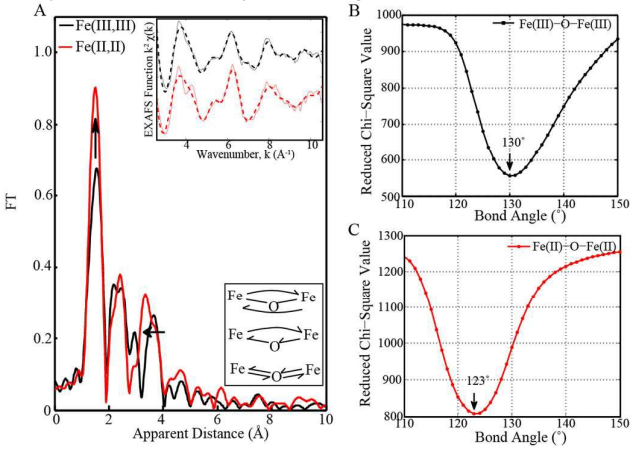

Figure 3 A. Fourier transforms of k^2-weighted Fe EXAFS of diiron(III,III) (black) and reduced diiron(II,II) (red) complexes. Top inset shows the comparison of their k^2-weighted Fe EXAFS of diiron(III,III) and diiron(II,II) complexes with corresponding EXAFS fits 3 and 7 in table S2. Multiple scattering paths for the Fe-O-Fe

View Article Online
DOI: 10.1039/C6CC08748E

unit are shown in the lower inset. Result of the Fe-O-Fe angle determination for **B**. diiron(III,III) and **C**. diiron(II,II)

The EXAFS spectra of the diiron(III,III) and diiron(II,II) complexes are shown in Figure 3A. A prominent peak is observed in the first coordination sphere corresponding to the Fe-N and Fe-O interactions due to aqua and methanol/methanolate solvent groups. EXAFS fits for both complexes for the first coordination sphere and the entire spectrum are shown in Table S1 and S2. The analysis of the first peak in the diiron(III,III) state resolves an averaged Fe-N/O distance at 2.05 Å. The analysis of the Fe-O-Fe bridging bond angle is carried out by creating a model accounting for the backscattering amplitude and phase shift of the Fe-O-Fe three atom system. This is achieved by fitting the experimental data over a range of Fe-O-Fe angles from 110˚/150˚ with 1 degree steps (Figure 3 B, C) with the best modelled fit having the least reduced chi square value. Changes detected in experimental EXAFS for the diiron(III,III) correlate well with data from XRD analysis[16] and multiple scattering simulations of DFT optimized coordinates(Figure S3). These findings show that theoretical geometry optimization methods for the diiron(III,III) state reproduce the experimental data well, and therefore can be reliably used for analysis of the reduced diiron(II,II) state. Interestingly, the diiron(II,II) compared to the diiron(III,III) state shows a reduction of the Fe-Fe distance from 3.72 to 3.58 Å and Fe-O-Fe bond angle from 130˚ to 123˚, in good agreement with DFT predicted trends (Table S2). Moreover, although EXAFS analysis shows that the averaged contribution of Fe-N/O bond distances of both diiron(III,III) and diiron(II,II) states within the first coordination sphere are similar, an increase in the amplitude of the first shell's peak is observed. This is most likely due to an increase in the bond distances of the Fe-O solvent groups upon reduction, due to a decrease in the charge state of the Fe centers, which can consequently contribute more positively to the grouped Fe-N interactions.

The spectroscopic characterization of light triggered charge accumulation at a catalytic site is a major hurdle primarily due to the intricate optical overlap or paramagnetic properties of all the constituents and intermediates present in a multicomponent system. In this work, we report on the use of tr-XAS to illustrate in "real-time" the two electron transfer steps in the light activation of a mulltimolecular diiron(III,III) methane monooxygenase model resulting in the formation of the diiron(II,II) charge accumulation state. Significantly, in the presence of the sacrificial electron donor, the formation of the long-lived diiron(II,II) state enables its structural determination. These findings are crucial toward increasing our understanding of charge separation dynamics in light driven activation of molecular catalysts.

This research used resources of the Advanced Photon Source and the Argonne Leadership User facility, U.S. DOE Office of Science User facilities, by Argonne National Laboratory (ANL) (contract no. DE-AC02-06CH11357). We are grateful for support from LABEX CHARMMAT. We thank Dr. Bostedt (ANL) for fruitful discussions. P.G.B thanks "La Caixa" foundation for a Ph.D grant.

Notes and references

1. L. H. Do, T. Hayashi, P. Moënne-Loccoz and S. J. Lippard, *J.Am.Chem.Soc.*, 2010, **132**, 1273-1275.
2. Y. Dong, S. Menage, B. A. Brennan, T. E. Elgren, H. G. Jang, L. L. Pearce and L. Que, *J.Am.Chem.Soc.*, 1993, **115**, 1851-1859.
3. B. A. Brennan, Q. Chen, C. Juarez-Garcia, A. E. True, C. J. O'Connor and L. Que, *Inorg.Chem.*, 1991, **30**, 1937-1943.
4. X. Liu, Y. Ryabenkova and M. Conte, *Phys.Chem.Chem.Phys.*, 2015, **17**, 715-731.
5. M. Merkx, D. A. Kopp, M. H. Sazinsky, J. L. Blazyk, J. Muller and S. J. Lippard, *J.Am.Chem.Soc.*, 2001, **40**, 2782-2807.
6. A. Trehoux, J.-P. Mahy and F. Avenier, *Coord.Chem.Rev.* 2016, **322**, 142-158.
7. L. Que, *Acc.Chem.Res.*, 2007, **40**, 493-500.
8. J. G. DeWitt, J. G. Bentsen, A. C. Rosenzweig, B. Hedman, J. Green, S. Pilkington, G. C. Papaefthymiou, H. Dalton, K. O. Hodgson and S. J. Lippard, *J. Am. Chem. Soc.*, 1991, **113**, 9219-9235.
9. A. Ericson, B. Hedman, K. O. Hodgson, J. Green, H. Dalton, J. G. Bentsen, R. H. Beer and S. J. Lippard, *J. Am. Chem. Soc.*, 1988, **110**, 2330-2332.
10. R. Davydov, A. M. Valentine, S. Komar-Panicucci, B. M. Hoffman and S. J. Lippard, *Biochemistry*, 1999, **38**, 4188-4197.
11. B. E. Sturgeon, P. E. Doan, K. E. Liu, D. Burdi, W. H. Tong, J. M. Nocek, N. Gupta, J. Stubbe, D. M. Kurtz, S. J. Lippard and B. M. Hoffman, *J.Am.Chem.Soc.*, 1997, **119**, 375-386.
12. S. Pulver, W. A. Froland, B. G. Fox, J. D. Lipscomb and E. I. Solomon, *J.Am.Chem.Soc.*, 1994, **116**, 4529-4529.
13. S. C. Pulver, W. A. Froland, J. D. Lipscomb and E. I. Solomon, *J.Am.Chem.Soc.* 1997, **119**, 387-395.
14. J. G. DeWitt, A. C. Rosenzweig, A. Salifoglou, B. Hedman, S. J. Lippard and K. O. Hodgson, *Inorg. Chem.*, 1995, **34**, 2505-2515.
15. L. Shu, J. C. Nesheim, K. Kauffmann, E. Münck, J. D. Lipscomb and L. Que, *Science*, 1997, **275**, 515-518.
16. F. Avenier, C. Herrero, W. Leibl, A. Debois, R. Guillot, J.-P. Mahy and A. Aukauloo, *Angew.Chem.Int.Ed*, 2013, **52**, 3634-3637.
17. C. Herrero, J. L. Hughes, A. Quaranta, N. Cox, A. W. Rutherford, W. Leibl and A. Aukauloo, *Chem.Commun.*, 2010, **46**, 7605-7607.
18. C. Herrero, A. Quaranta, W. Leibl, A. W. Rutherford and A. Aukauloo, *Energy Environ Sci*, 2011, **4**, 2353-2365.
19. W. Iali, P.-H. Lanoe, S. Torelli, D. Jouvenot, F. Loiseau, C. Lebrun, O. Hamelin and S. Ménage, *Angew.Chem.Intd.Ed*, 2015, **54**, 8415-8419.
20. E. I. Solomon, A. Decker and N. Lehnert, *Proc.Natl.Acad.Sci.*, 2003, **100**, 3589-3594.
21. L. X. Chen and X. Zhang, *J.Phys.Chem.Lett.*, **4**, 4000-4013.
22. D. Moonshiram, A. Guda, L. Kohler, A. Picon, S. Guda, C. S. Lehmann, X. Zhang, S. H. Southworth and K. L. Mulfort, *J.Phys.Chem.C.*, 2016, **120**, 20049-20057.
23. D. Moonshiram, C. Gimbert-Suriñach, A. Guda, A. Picon, C. S. Lehmann, X. Zhang, G. Doumy, A. M. March, J. Benet-Buchholz, A. Soldatov, A. Llobet and S. H. Southworth, *J.Am.Chem.Soc.*, 2016, **138** ,10586–10596
24. C. Bressler and M. Chergui, *Annu. Rev. Phys. Chem*, 2010, **61**, 263-282.
25. J. Cho, S. Jeon, S. A. Wilson, L. V. Liu, E. A. Kang, J. J. Braymer, M. H. Lim, B. Hedman, K. O. Hodgson, J. S. Valentine, E. I. Solomon and W. Nam, *Nature*, 2011, **478**, 502-505.
26. T. E. Westre, K. E. Loeb, J. M. Zaleski, B. Hedman, K. O. Hodgson and E. I. Solomon, *J. Am. Chem. Soc.*, 1995, **117**, 1309-1313.
27. T. E. Westre, P. Kennepohl, J. G. DeWitt, B. Hedman, K. O. Hodgson and E. I. Solomon, *J. Am. Chem. Soc.*, 1997, **119**, 6297-6314.
28. K. E. Loeb, T. E. Westre, T. J. Kappock, N. Mitic, E. Glasfeld, J. P. Caradonna, B. Hedman, K. O. Hodgson and E. I. Solomon, *J. Am. Chem. Soc.*, 1997, **119**, 1901-1915.

View Article Online
DOI: 10.1039/C6CC08748E

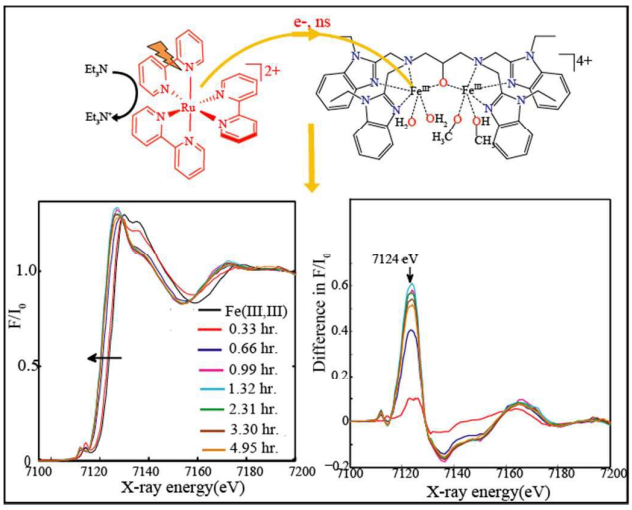

Photo-induced electronic and structural changes of an artificial analogue of methane monooxygenase enzyme are probed through time-resolved X-ray absorption spectroscopy.